

Understanding the electrochemical properties of Mg doped Li_2MnO_3 : First-principles calculations

Ziquan Zeng¹, Jianchuan Wang¹, Shiwei Zhang², Bo Han¹, Feng Dang³, Songlin Li¹, Yong Du¹

1 State Key Laboratory of Powder Metallurgy, Central South University,
410083, Changsha, China

2 College of Energy and Electrical Engineering, Qinghai University, 810016,
Xining, China

3 Key Laboratory for Liquid-Solid Structure Evolution and Processing of
Materials (Ministry of Education), Shandong University, 250061, Jinan, China

System	Lattice parameter (Å)		
	a	b	c
Li_2MnO_3	10.020	8.660	10.181
$\text{Mg}_{2b}\text{-Li}_2\text{MnO}_3$	10.024	8.663	10.186
$\text{Mg}_{4h}\text{-Li}_2\text{MnO}_3$	10.024	8.662	10.186

Table S1. Calculated lattice parameters of the supercells for pristine and Mg-doped Li_2MnO_3 .

System	Element	Atoms	Formation energy (eV)
$\text{Mg}_{2b}\text{-Li}_x\text{MnO}_3$	Li_{4h}	(a)	3.84
		(b)	3.42
		(c)	3.91
Li_xMnO_3	Li_{4h}	(a)	4.62
		(b)	4.59
		(c)	4.68

Table S2. Calculated formation energies of different Li_{4h} vacancies in Fig. S2.

System	x	Bader charge (e) of O						
		O1	O2	O3	O4	O5	O6	O
$\text{Mg}_{2\text{b}}\text{-Li}_x\text{MnO}_3$	2	-1.276 (-1.205)	-1.282 (-1.230)	-1.276 (-1.201)	-1.276 (-1.204)	-1.282 (-1.230)	-1.276 (-1.201)	-1.278 (-1.212)
		-1.236 (-1.176)	-1.199 (-1.112)	-1.190 (-1.109)	-1.236 (-1.176)	-1.199 (-1.112)	-1.190 (-1.109)	-1.208 (-1.132)
	1.75	-1.222 (-1.162)	-1.190 (-1.115)	-1.185 (-1.114)	-1.222 (-1.162)	-1.190 (-1.115)	-1.185 (-1.114)	-1.199 (-1.131)
		-1.140 (-1.055)	-1.190 (-1.091)	-1.140 (-1.055)	-1.140 (-1.055)	-1.190 (-1.090)	-1.140 (-1.055)	-1.156 (-1.067)
	1.25	-1.029 (-1.072)	-1.144 (-1.072)	-1.082 (-1.042)	-1.029 (-1.042)	-1.144 (-1.042)	-1.082 (-1.042)	-1.085 (-1.051)
		-1.302 (-1.230)	-1.239 (-1.201)	-1.238 (-1.204)	-1.302 (-1.230)	-1.239 (-1.201)	-1.239 (-1.204)	-1.260 (-1.212)
$\text{Mg}_{4\text{h}}\text{-Li}_x\text{MnO}_3$	2	-1.189 (-1.112)	-1.226 (-1.109)	-1.225 (-1.038)	-1.189 (-1.112)	-1.226 (-1.109)	-1.226 (-1.039)	-1.213 (-1.086)
		-1.189 (-1.115)	-1.209 (-1.114)	-1.123 (-0.877)	-1.189 (-1.115)	-1.209 (-1.114)	-1.209 (-0.877)	-1.173 (-1.036)
	1.75	-1.185 (-1.090)	-1.121 (-1.055)	-1.008 (-0.934)	-1.185 (-1.090)	-1.121 (-1.055)	-1.121 (-0.934)	-1.105 (-1.027)
		-1.083 (-1.090)	-1.033 (-1.050)	-1.014 (-0.906)	-1.083 (-1.090)	-1.033 (-1.050)	-1.033 (-0.906)	-1.049 (-1.015)
	1.25	-1.083 (-1.090)	-1.033 (-1.050)	-1.014 (-0.906)	-1.083 (-1.090)	-1.033 (-1.050)	-1.033 (-0.906)	-1.049 (-1.015)
		-1.083 (-1.090)	-1.033 (-1.050)	-1.014 (-0.906)	-1.083 (-1.090)	-1.033 (-1.050)	-1.033 (-0.906)	-1.049 (-1.015)

Table S3. Bader charges of O around Mg/Li in each delithiation stage. The values in brackets are the Bader charges of O anions in the undoped Li_2MnO_3 . The last column shows the averaged value of O.

System	x	Bader charge (e) of Mn						
		Mn1	Mn2	Mn3	Mn4	Mn5	Mn6	Mn
$\text{Mg}_{2\text{b}}\text{-Li}_x\text{MnO}_3$	2	+1.852 (+1.860)	+1.852 (+1.860)	+1.793 (+1.860)	+1.852 (+1.860)	+1.852 (+1.860)	+1.793 (+1.860)	+1.832 (+1.860)
	1.75	+1.843 (+1.852)	+1.860 (+1.864)	+1.868 (+1.876)	+1.860 (+1.864)	+1.843 (+1.852)	+1.856 (+1.861)	+1.855 (+1.861)
$\text{Mg}_{4\text{h}}\text{-Li}_x\text{MnO}_3$	1.5	+1.858 (+1.863)	+1.868 (+1.870)	+1.874 (+1.884)	+1.868 (+1.870)	+1.858 (+1.863)	+1.867 (+1.873)	+1.866 (+1.870)
	1.25	+1.868 (+1.873)	+1.868 (+1.874)	+1.882 (+1.882)	+1.868 (+1.874)	+1.868 (+1.873)	+1.882 (+1.882)	+1.873 (+1.876)
	1	+1.873 (+1.881)	+1.873 (+1.881)	+1.891 (+1.881)	+1.873 (+1.881)	+1.873 (+1.886)	+1.890 (+1.886)	+1.879 (+1.883)
	2	+1.787 (+1.860)	+1.787 (+1.860)	+1.822 (+1.860)	+1.822 (+1.860)	—	—	+1.806 (+1.860)
	1.75	+1.846 (+1.852)	+1.846 (+1.852)	+1.823 (+1.864)	+1.823 (+1.864)	—	—	+1.831 (+1.858)
	1.5	+1.863 (+1.863)	+1.863 (+1.863)	+1.837 (+1.870)	+1.837 (+1.870)	—	—	+1.850 (+1.866)
	1.25	+1.867 (+1.873)	+1.867 (+1.873)	+1.860 (+1.874)	+1.860 (+1.874)	—	—	+1.864 (+1.874)
	1	+1.874 (+1.879)	+1.874 (+1.879)	+1.867 (+1.881)	+1.867 (+1.881)	—	—	+1.871 (+1.881)

Table S4. Bader charges of Mn around Mg/Li in each delithiation stage. The values in brackets are the Bader charges of Mn anions in the undoped Li_2MnO_3 . The serial numbers for Mn are shown in Fig. S4 and the last column shows the averaged value of Mn.

System	x	Formation energy (eV)
Li_xMnO_3	2	2.61
	1.75	0.70
	1.5	0.34
	1.25	0.06
	1	-0.38
$\text{Mg}_{2b}\text{-Li}_x\text{MnO}_3$	2	3.63
	1.75	1.52
	1.5	1.27
	1.25	0.50
	1	0.06
$\text{Mg}_{4h}\text{-Li}_x\text{MnO}_3$	2	3.65
	1.75	1.36
	1.5	0.96
	1.25	0.45
	1	-0.02

Table S5. Average formation energy of O vacancies around the doping site at different delithiation stages in Li_xMnO_3 , $\text{Mg}_{2b}\text{-Li}_x\text{MnO}_3$ and $\text{Mg}_{4h}\text{-Li}_x\text{MnO}_3$.

Path	Diffusion barrier (eV)		
	Li_2MnO_3	$\text{Mg}_{2b}\text{-Li}_2\text{MnO}_3$	$\text{Mg}_{4h}\text{-Li}_2\text{MnO}_3$
2c-4h1	0.62	0.59	0.79
2c-4h2	0.88	0.78	0.82
2b-4h1	0.78	0.84	0.86

Table S6. The energy barrier for Li vacancy diffusion along path 2c-4h1, path 2c-4h2 and path 2b-4h1 in Li_2MnO_3 , $\text{Mg}_{2b}\text{-Li}_2\text{MnO}_3$ and $\text{Mg}_{4h}\text{-Li}_2\text{MnO}_3$.

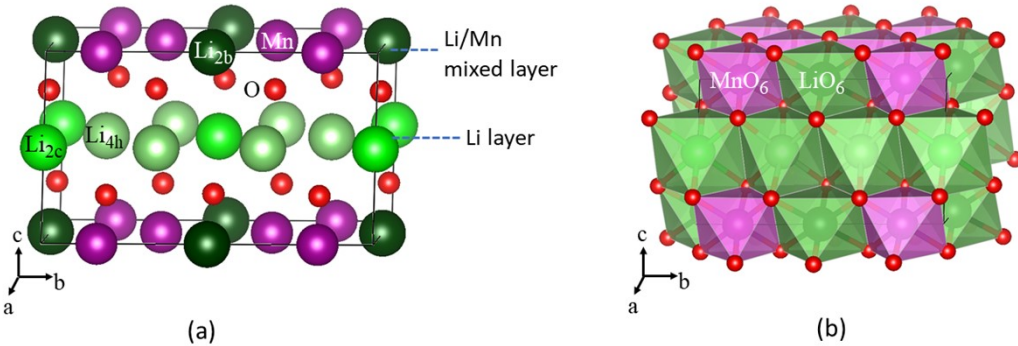


Fig. S1. (a) Monoclinic Li_2MnO_3 structure with a $\text{C}2/\text{m}$ space group and the atomic occupation positions of Li, Mn and O atoms. (b) Illustration of the MnO_6 and LiO_6 octahedra.

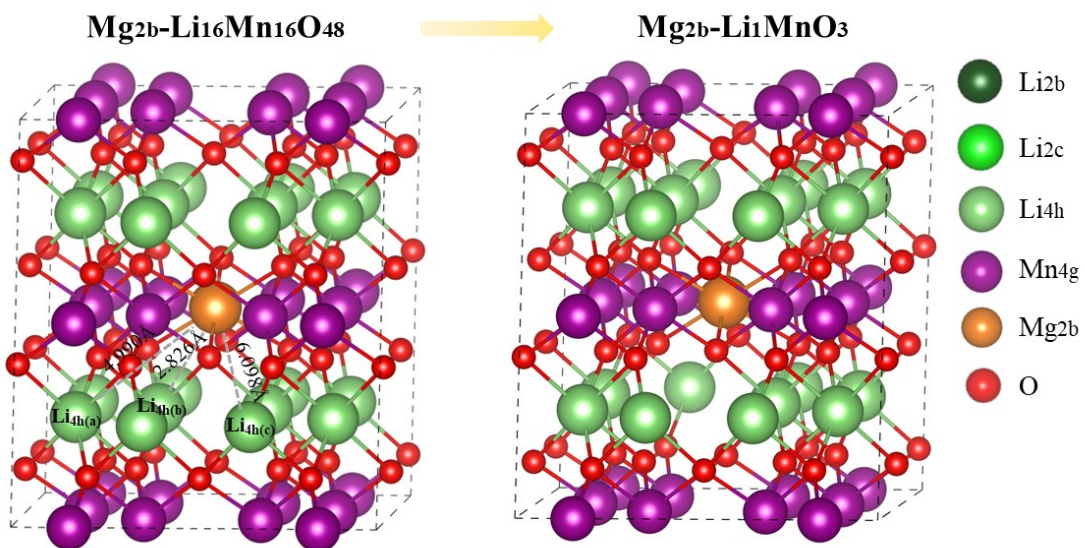


Fig. S2. The three un-equivalent 4h Li in the vicinity of doped Mg in $\text{Mg}_{2b}\text{-Li}_x\text{MnO}_3$.

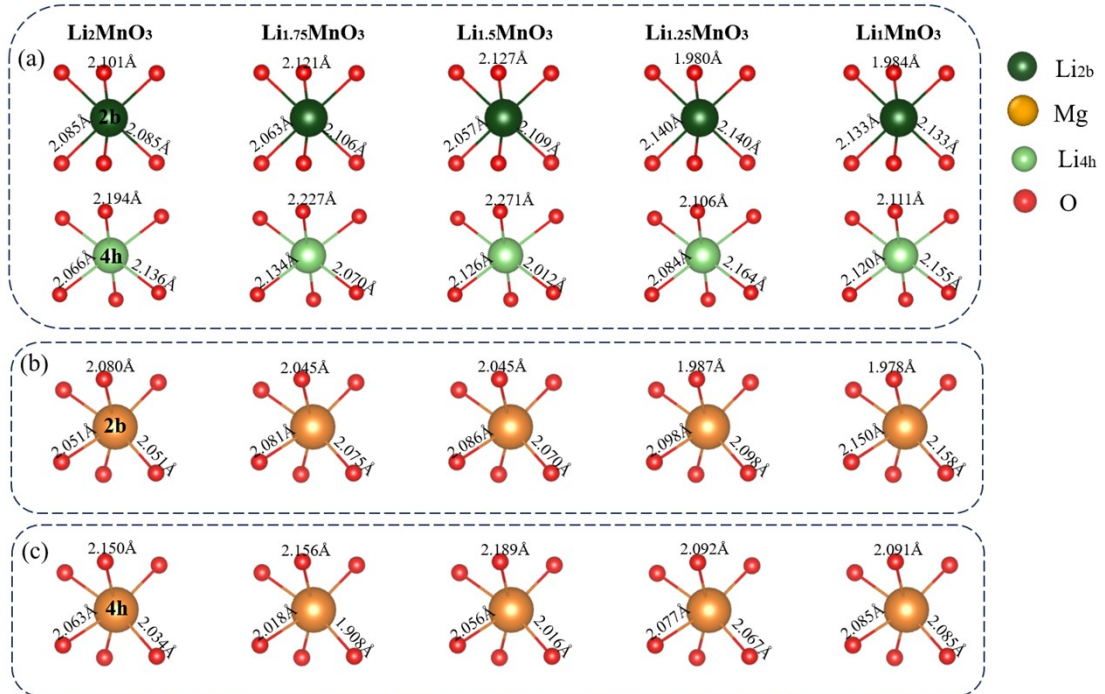


Fig. S3. Bond lengths of Li-O or Mg-O in (a) Li_xMnO_3 , (b) $\text{Mg}_{2\text{b}}\text{-Li}_x\text{MnO}_3$, and (c) $\text{Mg}_{4\text{h}}\text{-Li}_x\text{MnO}_3$ ($x = 2, 1.75, 1.5, 1.25$, and 1).

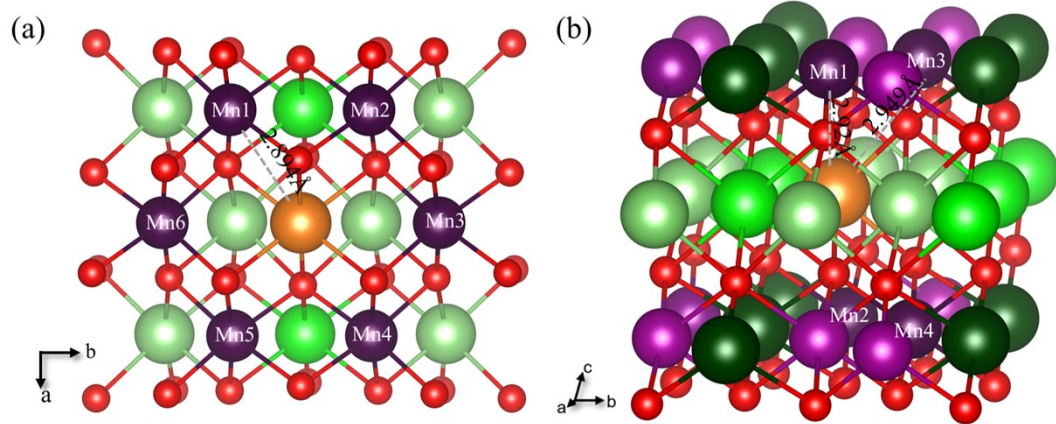


Fig. S4. Schematic shows the nearby by Mn ions of Mg in (a) $\text{Mg}_{2b}\text{-Li}_2\text{MnO}_3$ and (c) $\text{Mg}_{4h}\text{-Li}_2\text{MnO}_3$.

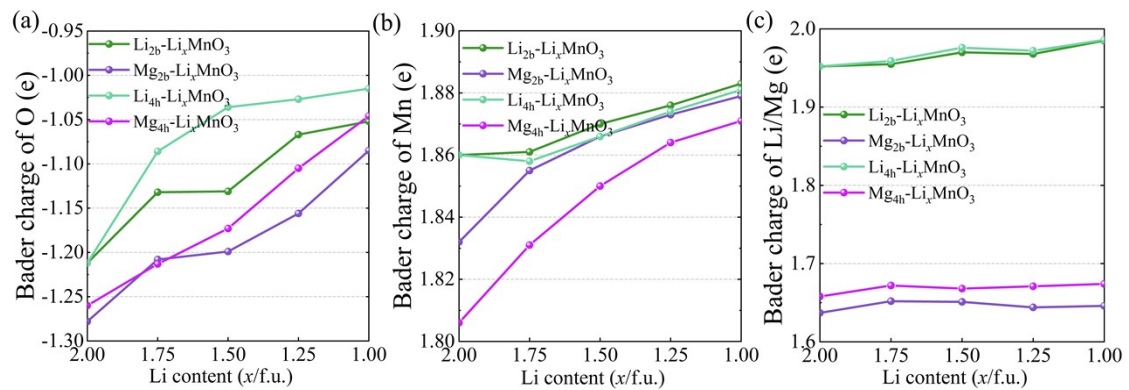


Fig. S5 The average Bader charge of (a) O in LiO_6 or MgO_6 octahedron, (b) Mn around Li or Mg, and (c) Li and doped Mg at different delithiation stages of Li_xMnO_3 ($x = 2, 1.75, 1.5, 1.25$, and 1).

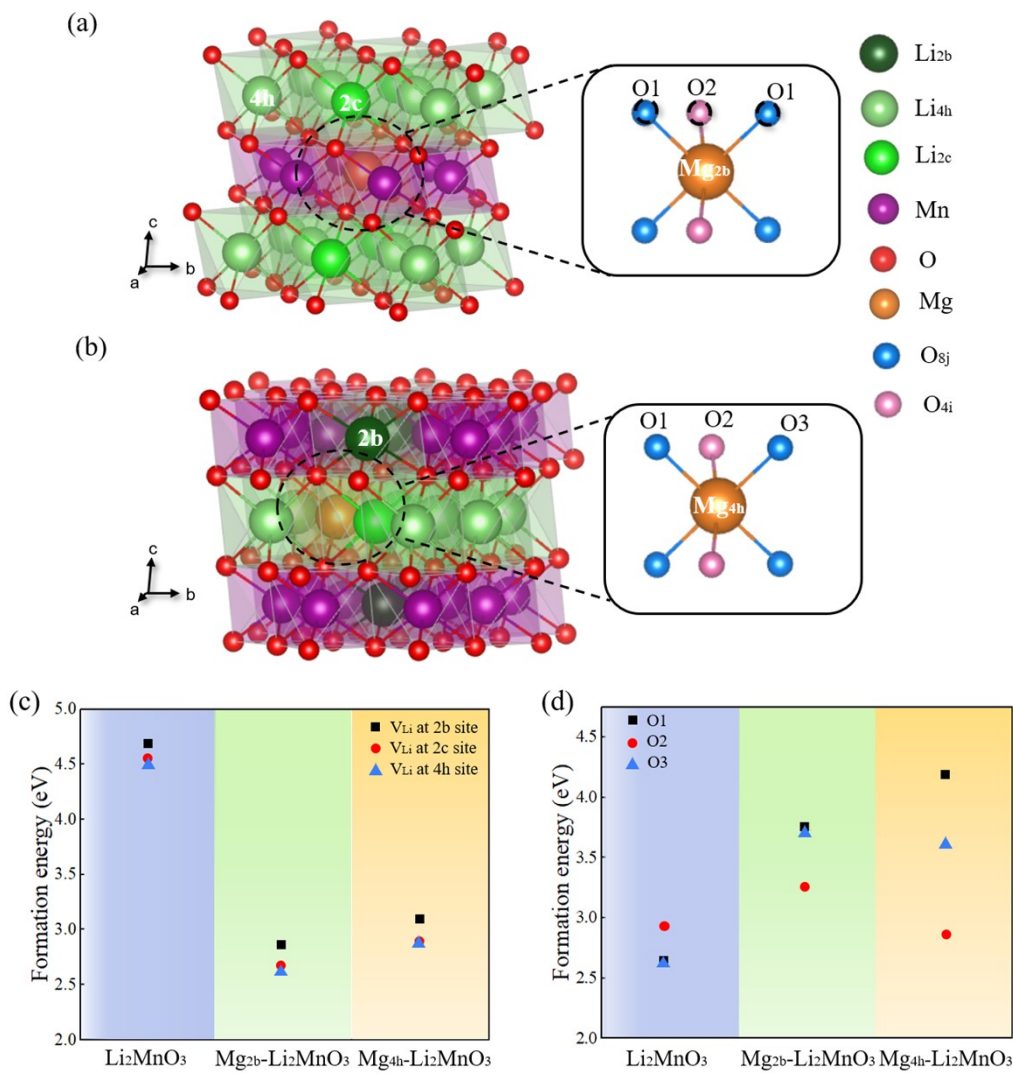


Fig. S6. (a) Illustration of different oxygen atoms (O_1 and O_2) near the doping site in the $\text{Mg}_{2\text{b}}\text{-Li}_2\text{MnO}_3$. (b) Illustration of different oxygen atoms (O_1 , O_2 , and O_3) near the doping site in the $\text{Mg}_{4\text{h}}\text{-Li}_2\text{MnO}_3$. (c) Formation energies of different Li vacancies in pure and Mg doped Li_2MnO_3 . (d) Formation energies of different O vacancies in pure and Mg doped Li_2MnO_3 .